

PREDICTION OF TEMPERATURE INSIDE A REFRIGERATED CONTAINER IN THE PRESENCE OF PERISHABLE GOODS

Javier Palafox-Albarrán, Reiner Jedermann and Walter Lang
Institute of Microsensors Actuators and Systems (IMSAS), University of Bremen
Otto Hahn Allee NW1, D-28359 Bremen, Germany

Keywords: System Identification, Temperature, Organic Heat, Feedback-hammerstein.

Abstract: This paper presents an alternative method to predict the temperature profile in a spatial point of the interior of a refrigerated container with the aim of improving the logistics of perishable goods. A SISO gray-box model in which the organic heat is represented by a non-linear feedback system and the cooling process represented by a linear system is proposed. Parameter adaptation and prediction algorithms for the model are modified to reduce the matrix dimensions, implemented in Matlab and applied to experimental data for validation. Apart from being highly accurate, the predictions comply with the desired figures of merit for the implementation in wireless sensor nodes, such as high robustness against quantization and environmental noise. Simulation results concludes that if the cargo emits organic heat, the proposed model is faster and more accurate than the linear models.

1 INTRODUCTION

Research has been done in the past to estimate the temperature profile inside refrigerated containers. Several options have been investigated: mathematical approaches as presented in (Shaik, 2007), K- ϵ models as proposed in (Rouaud, 2002), and several numerical models as reviewed in (Smale, 2006). With the exception of (Moureh, 2004), in which the effect of the pallets is considered; usually the focus is put on the cold air flow as the main factor governing the temperature pattern inside a container and the effects due the cargo presence is sub estimated.

To take into account the effect of the cargo in the temperature, in (Babazadeh, 2008) it is proposed the use of wireless sensor nodes (WSN) to measure the ambient parameters in the surroundings of a spatial point of interest and the use of system identification to estimate the parameters of a linear Multi-Input Single-Output (MISO) system. It concluded that in order to have a good estimation, it is necessary to have a high number of training samples and many inputs to the system.

In this paper an alternative Single-Input Single-Output (SISO) grey-box model is presented to predict the temperature inside the container under the presence of perishable goods with the aim of reducing the complexity and preserving the accuracy. The proposed model provides a meaningful description of the factors involved in the physical system including the effect of transporting living goods such as fruits and vegetables. The starting point is based on the physical relations; subsequently, a tuning parameter for the specific case of bananas is found by simulations.

2 MODEL OF THE SYSTEM

The factors affecting the temperature distribution inside a refrigerated container are illustrated in Figure 1. The cold air flows from bottom to top through the gratings in the floor and through the spaces between the pallets, and eventually it is drawn off the channel between the pallets and the container ceiling.

A naive representation of the container can be done by a SISO linear dynamic system in which the input is the air supply and the output is the spatial

point of interest. However, in reality it is only a simple model of the main contributor to the temperature pattern, the air flow. Several other factors affect the speed of the cooling down.

To improve the accuracy of the model, other contributors are considered as well: first is the heat, produced by respiration of living goods such as fruits and vegetables; second is the thermal loss, affecting the correct cooling of the goods; finally, unpredictable temperature variations due to highly changing external climatic conditions during transportation.

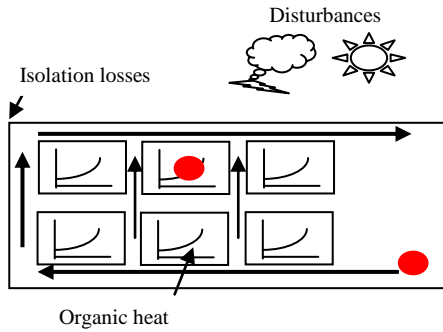


Figure 1: Factors affecting the temperature inside a refrigerated container.

The linear SISO black-box model representing the air flow is represented mathematically by a linear dynamic system H , which in the discrete domain is given by the Equation 1.

$$H(q^{-1}) = \frac{q^{-1}B(q^{-1})}{A(q^{-1})} \quad (1)$$

Where n_a and n_b are the orders of the system polynomials, $b_1 \dots b_{n_b}, a_1 \dots a_{n_a}$ are the polynomial coefficients, and q is the delay operator in discrete domain.

An attenuator, α , models the isolation losses of the air supply temperature and is modeled to affect the input of the dynamic system. The external climatic conditions are unknown in advance, therefore considered a statistical process. The output of the Moving Average (MA) process, which is in fact white noise (WN) filtered by the filter C represented in Equation 2 added to the output of the dynamic system, models them.

$$C(q^{-1}) = 1 + c_1 q^{-1} + \dots + c_{n_c} q^{-n_c} \quad (2)$$

To model the organic heat, it is necessary to use experimental data. Figure 2 (Mercantila, 1989) shows a family of curves for organic heat in the case of bananas. A proportional relationship between of the organic heat and the ripening state is observed.

Equation 3 represents the organic heat relation with respect to the temperature. P_{fruit} is the heat production in Watts, γ is a constant which is fixed for a certain type of fruit and ripening-state in $1/^\circ\text{C}$, T is the fruit temperature in $^\circ\text{C}$, and β is a scaling factor which depends of the amount of food and is given in kilograms.

$$P_{fruit} = \beta e^{\gamma T} \quad (3)$$

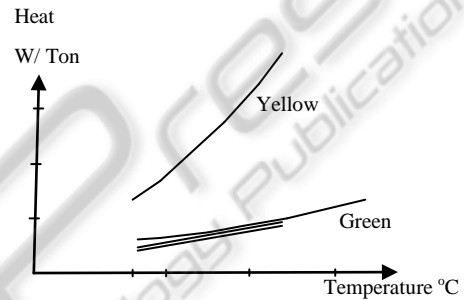


Figure 2: Heat Production of bananas.

Finally, the block diagram to represent the input-output relations of all the factors is built. It is shown in Figure 3. The air flow dynamics are represented as a feed-forward block as it is the most important contributor. The isolation losses affect the correct cooling of the goods before the dynamic system and the noise effect has an additive effect on the output.

The contribution of the organic heat depends on the cooling temperature inside the container. Simultaneously, it has a small additive effect in the input of the linear dynamic system as the air flows through the pallets and is slightly warmed. It is represented by a static exponential feedback. The resulting block diagram, in which a linear dynamic system has a non-linear feedback corresponds to a Feedback-Hammerstein (FH) configuration (Guo, 2004).

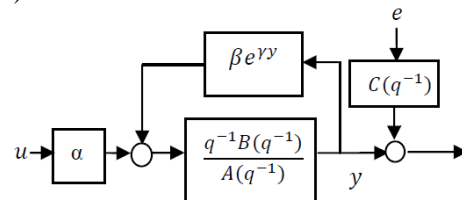


Figure 3: Model of the system.

3 PARAMETER ADAPTATION ALGORITHM

In (Guo, 2004) a Parameter Adaptation Algorithm (PAA) was developed to identify the parameter-set of a FH system. It uses an intermediate variable $\tilde{y}(t)$ and converts the non-linear system into a pseudo-linear one. Its principal advantage is that the conventional recursive matrix-based linear system identification algorithms as those presented in (Landau, 2005) can be applied to estimate the parameter matrix Θ . The recursive form of those algorithm is given by Equation 4. Where $\varepsilon(t)$ is the prediction error as described in Equation 5, $P(t+1)$ is an adaptation matrix to perform the minimization of ε using Recursive Least Squares method, and $\varphi(t)$ is the observation matrix that contains the input and the output data. $\lambda(t+1)$ in Equation 6 is the so called Forgetting Factor (FF).

$$\Theta(t+1) = \Theta(t) + (P(t+1)\varphi(t))^T \varepsilon(t) \quad (4)$$

$$\varepsilon(t) = y(t) - \Theta(t)^T \varphi(t-1) \quad (5)$$

$$P(t+1) = \frac{P(t) - P(t)\varphi\varphi^T \left(\frac{P(t)}{\varphi^T P \varphi + \lambda(t+1)} \right)}{\lambda(t+1)} \quad (6)$$

$$\lambda(t+1) = \lambda_o * \lambda(t) + 1 - \lambda_o \quad (7)$$

Guo considers the non-linearity as a polynomial of order l as shown in Equation 8; however, the dimensions of the matrices in the algorithm would be significantly too large to be applied in platforms where power consumption is an important figure of merit.

$$\eta(y(t)) = \sum_{k=0}^l \mu_k y^k(t) \quad (8)$$

To reduce the dimensions of the matrices, was proposed the use of the exponential Equation in Equation 3 instead. γ is to be determined and it remains constant, while β is a parameter to be identified as it depends on the amount of fruit being transported. The linear term of the Equation 8 needs to be extracted to be included in the polynomial $A^*(q^{-1})$ of the equivalent SISO pseudo-linear system. Expanding it into a Taylor series and rearranging, the summation of the non-linear coefficients of the exponential function can be calculated using Equation 9. The non-linear coefficients and an offset are on the left hand of the equation.

$$\sum_{k=2}^{\infty} \frac{(\gamma y(t))^k}{k!} + 1 = e^{\gamma y(t)} - \gamma y(t) \quad (9)$$

The equivalent pseudo-linear system for an exponential non-linearity is shown in Equation 10.

$$A^*(q^{-1})y(t) = b_1 \alpha u(t) + b_1 \beta e^{\gamma y(t)} - b_1 \beta y(t) + \frac{B^*(q^{-1})}{b_1} \tilde{y}(t) + C(q^{-1})e(t) \quad (10)$$

The resulting coefficients of the polynomials $A^*(q^{-1})$ and $B^*(q^{-1})$ are given by Equation 11 and 12.

$$a_k^* = a_k - (\beta \gamma) b_k \quad (11)$$

$$B^*(q^{-1}) = b_2 q^{-2} + \dots + b_{n_b} q^{-n_b} \quad (12)$$

And the intermediate variable is shown by Equation 13.

$$\tilde{y}(t) = b_1 [a u(t) + \beta (e^{\gamma y(t)} - \gamma y(t))] \quad (13)$$

The choice of the forgetting factor in the algorithm is often critical. In theory, it must be one that converges. On the other hand, if it is less than one the algorithm becomes more sensitive and the estimated parameter changes quickly making the convergence faster. A more complex solution is to allow it to vary with time, lower than one at the beginning but tending to one.

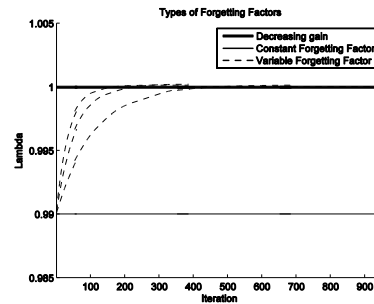


Figure 4: Types of forgetting factors.

Figure 4 illustrates three different types of FF. The first case is obtained by making λ_o , and $\lambda(t)$ in Equation 7 equal to one. It is called Decreasing Gain (DG). In the second case, the Constant Forgetting Factor (CFF) $\lambda(t)$ is set to a value smaller than one and λ_o set to one. Finally, the Variable Forgetting Factor (VFF) uses a value of λ_o smaller than one and recalculates $\lambda(t)$ for each iteration.

Table 1: Elements of the elements in the algorithm matrices.

Symbol	Arrangement of the elements into the matrices
$\varphi(t)$	$[-y(t) \cdots -y(t - n_a + 1), u(t - 1), (e^{\gamma y(t)} - \gamma y(t)), \tilde{y}(t - 1) \dots \tilde{y}(t - n_b), \varepsilon_n(t) \cdots \varepsilon_n(t - n_c + 1)]$
$\Theta^T(t)$	$[a_1^* \dots a_{n_a}^*, b_1 \alpha, \beta b_1, b_2/b_1 \dots b_{n_b}/b_1, c_1 \dots c_{n_c}]$
$\varphi_{pred}(t)$	$[-y_{pred}(t) \cdots -y_{pred}(t - n_a + 1), u(m), (e^{\gamma y_{pred}(t)} - \gamma y_{pred}(t)), \tilde{y}_{pred}(t - 1) \dots \tilde{y}_{pred}(t - n_b)]$
$\Theta^T(m)$	$[a_1^* \dots a_{n_a}^*, b_1 \alpha, \beta b_1, b_2/b_1 \dots b_{n_b}/b_1]$

4 PREDICTION ALGORITHM

The predictions are made using the estimated parameters in the model. Figure 5 shows experimental data sets from a container transporting bananas. It can be observed how the air supply is kept constant after some days. For the prediction algorithm, $u(t)$ is set to the value of the last sampled input temperature of the parameter adaptation process. Similarly, the initial predicted output value is set to the last acquired value of the output. Equation 14 to 17 describes the prediction algorithm. m is the number of iterations used for the PAA.

$$u_{pred}(t) = u(m) \quad (14)$$

$$y_{pred}(m) = y(m) \quad (15)$$

$$y_{pred}(t) = \Theta^T(m) \varphi_{pred}(t-1) \quad (16)$$

$$\tilde{y}_{pred}(t) = b_1 [\alpha u(m) + \beta (e^{\gamma y_{pred}(t)} - \gamma y_{pred}(t))] \quad (17)$$

5 DETERMINATION OF γ

In considering a linear system, an exponential discrete time decaying system like the one presented in Figure 5 can be described as of the order of one with its unique pole on the real positive axis. The closer the pole to one the higher the delay of the system.

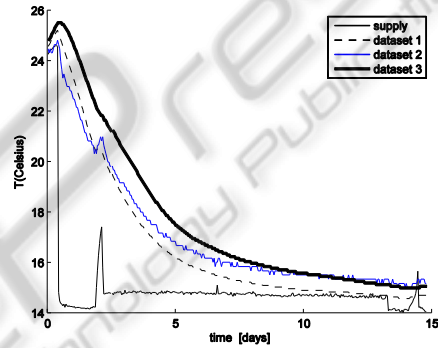
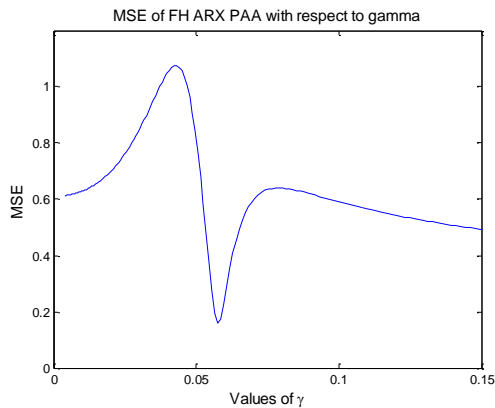


Figure 5: Banana data sets.

To find a trustworthy γ parameter that characterizes the respiration heat of bananas. The presented Feedback-Hammerstein model of linear order one and the FH parameter adaptation and prediction algorithms are run using given experimental data sets. The Mean Squared Error (MSE) of the prediction over n samples, equivalent to fifteen days, is stored for several values of γ and fixed number of training days. If the stored values of the MSE are plotted, the local minimums are determined by the observation of the MSE vs. γ curves. In Figure 6, it can be seen that in the above mentioned plot for five days of training and for the data set 1, a local minimum exists for a value γ of 0.0587.

$$MSE = \frac{1}{n} \sum_{t=m}^n (y_{real}(t) - y_{pred}(t))^2 \quad (18)$$


 Figure 6: Prediction accuracy vs. γ .

6 RESULTS

For validation of the model and algorithms several figures of merit are considered. The accuracy and the speed of convergence are of paramount importance; however, quantization and noise robustness are also highly desirable for implementation in a WSN. Only the linear orders of one and two are considered to avoid computation of complex conjugate poles that would characterize oscillations.

To observe the speed of convergence and the accuracy of the predictions with respect to the number of training days, parameter estimation and a prediction in Matrix form are done (See Table 1) for a fixed number of training days. Subsequently, *MSE vs. Training days* graphs are plotted. Assuming a quantization level of 0.2°C , a Matlab script was written to assign the nearest value of the quantization grid to the input and the output datasets. The results of the predictions using the quantized datasets are overlapped with the results of non-quantized.

Similarly, to determine the noise robustness, MSE versus the signal to noise ratio (SNR) is plotted. Several noise levels of white noise were added to the output of the data set 1, and the resulting signals were applied to PAA and prediction algorithms with fixed number of training days.

$$\text{SNR}(\text{dB}) = 10 \log \left(\frac{P_{\text{signal}}}{P_{\text{noise}}} \right) \quad (19)$$

Simulations were done for two types of data sets. First, the experimental data of bananas were used to include the presence of organic heat. Secondly, the

data sets corresponding to a cheese experiment, which does not present organic heat, were considered. A summary of all simulation results is presented on Table 2.

6.1 FH vs. Linear Models in the Presence of Organic Heat

From the simulations it is observed in Figures 7 and 8 that if linear methods are applied to the banana datasets, the accuracy of the results for different sensor positions of are not sufficient. Quantization robustness is improved with the linear order of one and the speed of convergence is better using CFF. In the best of cases acceptable prediction accuracy can only be achieved after more than five days of training.

It is also observed in Figures 8 and 9 that FH identification algorithms are the best to achieve fast convergence speeds. In the best cases, less than 3 days of training is sufficient to achieve good predictions. However, the plots are made for the data from three days onwards to avoid the visualization of the effects in MSE due to the set point variations in the reefer supply temperature. Linear system orders of one are in all cases better than order of two, both in the speed of convergence and the quantization robustness. Decreasing Gain must be optimal to preserve the accuracy and the quantization robustness.

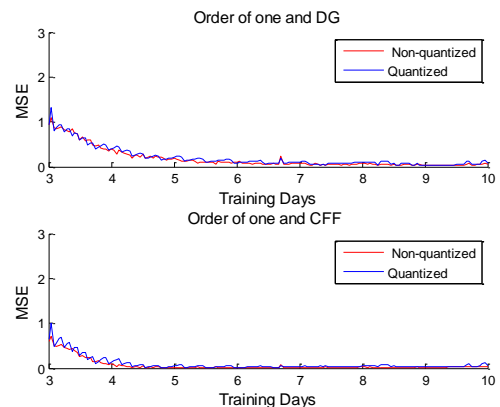


Figure 7: ARX of order one in the presence of organic heat.

Concerning the noise models, results of the simulation of Feedback-Hammerstein with MA process are worse than when modeled as white noise (WN). It affects the accuracy and the quantization robustness

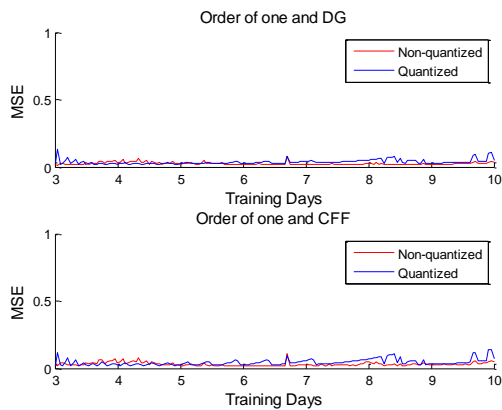


Figure 8: FH of order one in the presence of organic heat.

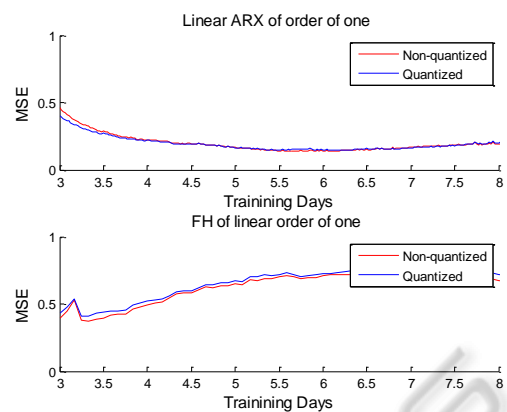


Figure 10: Comparison of FH and linear methods in the absence of organic heat.

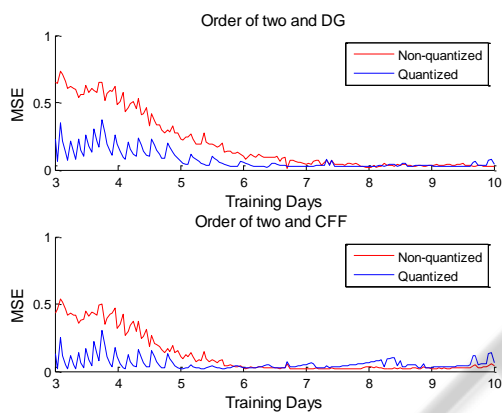


Figure 9: FH of order two in the presence of organic heat.

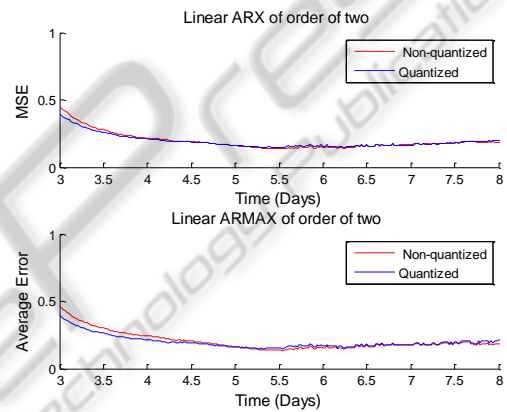


Figure 11: Comparison of linear methods with MA and WN models.

6.2 FH vs. Linear Models in the Absence of Organic Heat

In the case of cheese data set, the linear methods accuracy results are better than that of the Feedback-Hammerstein as can be observed in Figure 10. Modeling noise as white gives better quantization robustness than modeling it as MA process.

The use of forgetting factors does not have a big impact in the results of ARX predictions; however, Constant Forgetting Factor is slightly better for ARMAX predictions. Linear orders do not affect the simulated predictions, but an order of two is selected because it can model more accurately if the behavior of the system is not purely decaying.

6.3 Noise Robustness

The noise was added to validate FH and linear models; also for both of them the accuracy is compared with and without the MA model. Maximum Signal-to-Noise Ratio to obtain a good prediction is observed to be around 43 dB for all of them with the exception of ARX which has a maximum value of 47 Decibels as shown in Table 2.

6.4 Prediction Improvement

The described approach was originally developed based on an experiment in 2008 with records for 3 sensors (data set A). Two new data sets with 16 sensors each, which were recorded in 2009 (Jedermann, 2010) in two separate containers (data set B and C), were used to cross validate the approach.

Table 2: Summary of simulation results.

	Accuracy		Number of matrix elements	Convergence speed	Quantization Robustness	Critical SNR	Estimation for linear dataset
	Best Forgetting Factor	Best Linear order					
ARX	CFF	2	3	Bad	Good	47dB	Good
ARMAX	CFF	2	$3 + n_c$	Bad	Bad	43 dB	
FH and WN model	DG	1	3	Good	Good	43 dB	Bad
FH and MA model	DG	1	$3 + n_c$	Good	Bad	43 dB	

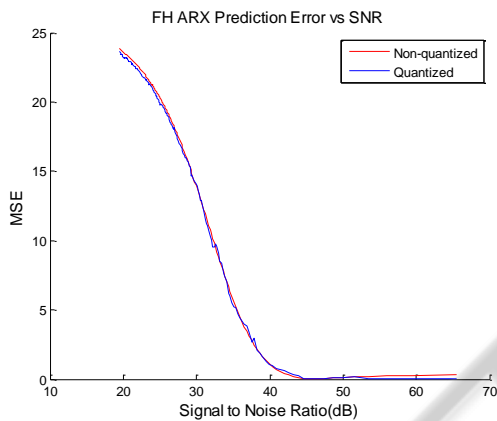


Figure 12: Noise Robustness for FH method

FH algorithm of linear order of one was applied to all data sets; neither quantization nor forgetting factor is used. For the initial parameter settings, the pole and zero of the feed-forward linear system was set to 0.9 and 0.0; β was set to 2.

The previously obtained value of γ equal to 0.0587 is used to predict the temperature inside the containers for many spatial positions. The results are compared to the predictions for the datasets shown in Figure 5 and resumed in Table 3. A good average is observed for the three containers; however, in some positions the predictions are not as accurate as is observed in the Maximum column.

 Table 3: MSE prediction results for a unique value of γ .

Container/Result	Maximum	Minimum	Average
Data set A	0.1893	0.0173	0.0778
Data set B	1.4558	0.0550	0.4130
Data set C	0.8888	0.0101	0.2798

A second approach is to select γ according to the position of the pallets inside the container. The method to find γ , described previously, is applied to all the new container datasets.

It is observed that an improvement in the accuracy of the predictions can be made if two different values of γ are selected: one for pallets close to the door-end, and one for pallets close to the reefer supply. In Table 4 it is resumed the prediction results if values of 0.0525 and 0.055 are set respectively.

 Table 4: MSE prediction results for values of γ according to the position inside the container.

Container/Result	Maximum	Minimum	Average
Data set A	0.1893	0.0173	0.0778
Data set B	0.4767	0.0279	0.0946
Data set C	0.5747	0.0201	0.1743

7 CONCLUSIONS

A model to represent the factors affecting the temperature inside a refrigerated container transporting perishable goods was proposed. It models the effect of organic heat using a static non-linear feedback system, the refrigeration by a linear dynamic feed-forward system, and the disturbances by stochastic processes. This complex model can provide an accurate description of the factors involved in the physical system.

The selected identification method was adapted specifically to reduce the dimensions of the matrices. The non-linear exponential function is used instead of a polynomial to preserve the simplicity of the parameter adaptation and the prediction algorithms. The disadvantage of the

simplification is that depending on the kind of fruits to be transported, it is required to tune the algorithm by a correct selection of γ which has to be known in advance. An improvement can be observed in the accuracy of the predictions if γ is set according to the position of the pallets inside the container.

From the simulation results it is concluded that the FH identification algorithm is efficient when the cargo emits organic heat. The method of FH of order 1 is optimal to achieve all figures of merit. It makes accurate predictions only after three days of training and maintains low dimensions of matrices.

However, if the linear method is applied to the banana datasets, a comparable accuracy can only be achieved after more than five days of training. Also, it is concluded that when the goods to transport are free of organic heat, such as in the case of cheese, it is preferable to use a linear system instead.

ACKNOWLEDGEMENTS

The authors would like to express their gratitude to Prof. Rainer Laur, Dirk Hentschel, Mehrdad Babazadeh, and Chanaka Lloyd for all their help.

This research was supported by the German Research Foundation (DFG) as part of the Collaborative Research Centre 637 "Autonomous Cooperating Logistic Processes". Further project information can be found at www.intelligentcontainer.com.

REFERENCES

Babazadeh, M., Kreowski, H.-J., Lang, W., 2008. Selective Predictors of Environmental Parameters in Wireless Sensor Networks. In International Journal of Mathematical Models and Methods in Applied Sciences Vol.2, pages 355-363.

Guo, F., 2004. A New Identification Method for Wiener and Hammerstein System. Ph.D. Thesis, Institut für Angewandte Informatik Forschungszentrum Karlsruhe, Karlsruhe.

Jedermann, R., Becker, M., Görg, C., Lang, W., 2010. Field Test of the Intelligent Container, In European Conference on Wireless Sensor Networks EWSN2010, 16-19 February 2010 in Coimbra, Portugal.

Landau, I.D., Zito G., 2006. Digital Control Systems: Design, identification and implementation. Springer. London, 1st edition.

Mercantila. 1989. Guide to food transport: fruit and vegetables. Mercantila Publ. Copenhagen.

Moureh J., Flick, D., 2004. Airflow pattern and temperature distribution in a typical refrigerated truck configuration loaded with pallet. In International Journal of Refrigeration, V. 27, Issue 5, pages 464-474.

Palafox J., 2009. Prediction of temperature in the transport of perishable goods based in On-line System Identification. M.Sc. Thesis, University of Bremen. Bremen.

Rouaud, O., Havet, M., 2002. Computation of the airflow in a pilot scale clean room using K- ϵ turbulence models, In International Journal of Refrigeration, Vol. 25, Issue 3, pages 351-361.

Shaikh, N. I., Prabhu, V., 2007. Mathematical modeling and simulation of cryogenic tunnel freezers. In Journal of Food Engineering, Vol. 80, Issue2, pages 701-710.

Smale, N. J., Moureh, J., Cortella, G., 2007. A review of numerical models of airflow in refrigerated food applications. In International Journal of Refrigeration, Vol. 29, Issue 6, pages 911-930.

LIST OF ABBREVIATIONS

ARMAX	Auto Regressive Moving Average with External input.
ARX	Auto Regressive with External input.
CFF	Constant Forgetting Factor
DG	Decreasing Gain
FF	Forgetting Factor
FH	Feedback Hammerstein
MA	Moving Average
MSE	Mean Squared Error
PAA	Parameter Adaptation
WN	Algorithm White Noise
WSN	Wireless Sensor Node